OPEN

Journal of Cerebral Blood Flow & Metabolism (2015) 35, 1169–1174

www.jcbfm.com

ORIGINAL ARTICLE

# Imaging *in vivo* glutamate fluctuations with [$^{11}$C]ABP688: a GLT-1 challenge with ceftriaxone

Eduardo R Zimmer[1,2,3], Maxime J Parent[1,2], Antoine Leuzy[1,2], Antonio Aliaga[4], Arturo Aliaga[1], Luc Moquin[5], Esther S Schirrmacher[4], Jean-Paul Soucy[4], Ivan Skelin[4], Alain Gratton[5], Serge Gauthier[2] and Pedro Rosa-Neto[1,2,4]

Molecular imaging offers unprecedented opportunities for investigating dynamic changes underlying neuropsychiatric conditions. Here, we evaluated whether [$^{11}$C]ABP688, a positron emission tomography (PET) ligand that binds to the allosteric site of the metabotropic glutamate receptor type 5 (mGluR5), is sensitive to glutamate fluctuations after a pharmacological challenge. For this, we used ceftriaxone (CEF) administration in rats, an activator of the GLT-1 transporter (EAAT2), which is known to decrease extracellular levels of glutamate. MicroPET [$^{11}$C]ABP688 dynamic acquisitions were conducted in rats after a venous injection of either saline (baseline) or CEF 200 mg/kg (challenge). Binding potentials ($BP_{ND}$) were obtained using the simplified reference tissue method. Between-condition statistical parametric maps indicating brain regions showing the highest CEF effects guided placement of microdialysis probes for subsequent assessment of extracellular levels of glutamate. The CEF administration increased [$^{11}$C]ABP688 $BP_{ND}$ in the thalamic ventral anterior (VA) nucleus bilaterally. Subsequent microdialysis assessment revealed declines in extracellular glutamate concentrations in the VA. The present results support the concept that availability of mGluR5 allosteric binding sites is sensitive to extracellular concentrations of glutamate. This interesting property of mGluR5 allosteric binding sites has potential applications for assessing the role of glutamate in the pathogenesis of neuropsychiatric conditions.

*Journal of Cerebral Blood Flow & Metabolism* (2015) **35,** 1169–1174; doi:10.1038/jcbfm.2015.35; published online 25 March 2015

**Keywords:** [$^{11}$C]ABP688; ceftriaxone; glutamate; GLT-1; mGluR5; positron emission tomography

## INTRODUCTION

Glutamate is the major excitatory neurotransmitter in the mammalian brain, acting on ionotropic (AMPAr, KAr and NMDAr) and metabotropic (mGluRs) receptors. The ionotropic receptors produce fast-acting excitatory effects, while mGluRs (G protein-coupled receptors) have a crucial role in the modulation of glutamatergic neurotransmission.[1] Since glutamate is not degraded in the extracellular compartment, two major astrocytic transporters, GLT-1 (EAAT2) and GLAST (EAAT1), remove glutamate from the synapses and provide the regulation necessary to orchestrate receptor excitability.[2] The disruption of this fine-tuning mechanism causes hyperactivation of glutamatergic receptors, a well-established detrimental scenario termed excitotoxicity, which is described as a fundamental player in the pathophysiology of several neurologic and psychiatric disorders.[3,4] Due to the glutamatergic system's involvement in a large array of neuropsychiatric conditions, techniques allowing for noninvasive *in vivo* estimation of glutamatergic neurotransmission are highly desirable.

Positron emission tomography (PET) is an imaging technique that allows for the *in vivo* measurement of biologic processes such as receptor availability or fluctuations of endogenous neurotransmitters.[5] Advances in pharmacology have allowed for the development of PET radiopharmaceuticals targeting allosteric binding sites of the metabotropic glutamate receptor type 5 (mGluR5).[6] Previous PET studies showed that pharmacological challenges with *N*-acetylcysteine, a facilitator of the cysteine-glutamate antiporter that increases the release of nonsynaptic glutamate, produced a decrease in the binding of the PET radiopharmaceutical [$^{11}$C]ABP688, an allosteric and highly selective mGluR5 antagonist, in baboons[7] and in rhesus monkeys.[8] In contrast, a recent study showed no effect of *N*-acetylcysteine on [$^{11}$C]ABP688 binding in rats.[9] In fact, little is known regarding noncompetitive interactions between glutamate and the availability of mGluR5 allosteric binding sites. Although important, none of the previous studies tested whether pharmacologically induced declines of extracellular glutamate concentrations increased the availability of mGluR5 allosteric binding sites.

With this in mind, we used ceftriaxone (CEF)—a potent GLT-1 activator, which decreases extracellular levels of glutamate[10–12]—to investigate whether the PET radiopharmaceutical [$^{11}$C]ABP688 is sensitive to declines in extracellular glutamate concentrations.

## MATERIALS AND METHODS

### Animals

Sprague-Dawley rats ($n = 5$, 392.10 ± 58.69 g) were scanned twice within 2 to 7 days (baseline and challenge). The scanning was conducted between

[1]Translational Neuroimaging Laboratory (TNL), McGill Center for Studies in Aging, Douglas Mental Health University Institute, Verdun, Quebec, Canada; [2]Alzheimer's Disease Research Unit, McGill Centre for Studies in Aging, McGill University, Montreal, Quebec, Canada; [3]Department of Biochemistry, Federal University of Rio Grande do Sul (UFRGS), Porto Alegre, RS, Brazil; [4]Montreal Neurological Institute (MNI), Montreal, Quebec, Canada and [5]Department of Psychiatry, Douglas Hospital Research Centre, McGill University, Montreal, Quebec, Canada. Correspondence: Dr P Rosa-Neto, McGill Center for Studies in Aging, 6825 LaSalle Boulevad, Montreal, H4H 1R3 Quebec, Canada.
E-mail: pedro.rosa@mcgill.ca

This work was supported by the Canadian Institutes of Health Research (CIHR) [MOP-11-51-31], the Allan Tiffin Foundation, the Alzheimer's Association [NIRG-08-92090], the Fonds de recherche du Québec – Santé (FRSQ; chercheur boursier), the Conselho Nacional de Desenvolvimento Científico e Tecnológico (CNPq, Brazil), fundação de Amparo à Pesquisa do Rio Grande do Sul (Fapergs, Brazil), and INCT for Excitotoxicity and Neuroprotection/CNPq.
Received 20 August 2014; revised 16 December 2014; accepted 30 December 2014; published online 25 March 2015

1030 h and 1330 h. Additional Sprague-Dawley rats ($n = 6$, 452.10 ± 68.69 g) were used for microdialysis. The microdialysis was conducted between 1030 h and 1530 h. Animals were kept in a room with controlled temperature (21°C) under a 12-hour light/12-hour dark cycle (lights on 0800 h), with *ad libitum* access to food and water. All procedures were performed according the Guide to the Care and Use of Experimental Animals (Ed2) of the Canadian Council on Animal Care. The protocols for PET imaging, surgery, and microdialysis were approved by the Animal Care Committee of McGill University (Montreal, QC, Canada).

### Radiosynthesis, Pharmaceuticals, and Imaging Procedures

[$^{11}$C]ABP688 was synthesized as described previously.[13] The mean specific radioactivity for the baseline was 12.35 ± 5.75 TBq/mmol and for the challenge 12.74 ± 2.49 TBq/mmol (mean ± s.d.). The PET acquisitions were performed using a Concorde MicroPET R4 scanner (Siemens-CTI, Knoxville, TN, USA), as previously described by Elmenhorst.[13] Rats were placed in a prone position with the head immobilized by both the body holder and the nose cone of the anesthesia system (2% isoflurane at 0.5 L/min oxygen flow). The brain was positioned in the center of the field of view. A 10-min transmission scan with a rotating [$^{57}$Co] point source was acquired to correct for attenuation followed by the 60-minute emission scan. For the baseline, they received a tail vein injection of saline 30 minutes before the scan (Figure 1A). For the challenge, they received a tail vein injection of CEF 200 mg/kg 30 minutes before the scan (Figure 1B). Subsequently, [$^{11}$C]ABP688 was administered as a bolus injection (0.2 mL) into the tail vein. Respiratory rate, heart rate, and body temperature were monitored throughout the scan (Biopac Systems MP150, Goleta, CA, USA). Mean injected radioactivity was 17.02 ± 2.89 MBq for baseline and 16.62 ± 4.31 MBq for challenge (mean ± s.d.). Ceftriaxone was dissolved in saline (200 mg/kg).

### Image Reconstruction, Analysis, Processing, and Estimation of Binding Parameters

Images were reconstructed using an MAP (maximum *a posteriori*) algorithm, normalized and corrected for scatter, dead time, and decay. Imaging analysis was conducted using minctools (http://www.bic.mni.mcgill.ca/ServicesSoftware/). Time-averaged tissue-radioactivity images were manually coregistered to a standard rat histologic template.[14] The image outcome measure, nondisplaceable binding potential ($BP_{ND}$), was estimated using the simplified reference tissue model,[15] with the cerebellum as a reference region due to its low [$^{11}$C]ABP688 binding.[13] [$^{11}$C]ABP688 $BP_{ND}$ was estimated for every dynamic scan, with resulting images convolved using a 2.4-mm Gaussian kernel. The PET images were corrected for motion by realigning each frame to a reference frame using mutual information as the cost function.[16] For detailed information regarding PET methodology (including error analysis, parameter sensitivity analysis, and scan duration) and simplified reference tissue model analytical details, see Elmenhorst.[13]

### Microdialysis Surgery, Procedure, and Histology

Rats were anesthetized with sodium isoflurane (2% isoflurane at 0.5 L/min oxygen flow), and stereotaxically implanted with 22 gauge stainless steel guides into the left frontal cortex (FC), anteroposterior (AP): 4.20 mm, mediolateral (ML): 1.0 mm, dorsoventral (DV): 5.0 mm) and into the right thalamic ventral anterior (VA) (AP:– 1.88 mm, ML: 2.0 mm, DV: 6.5 mm) following Paxinos coordinates.[17] These cannulas were used to insert the microdialysis probes into the target sites. Cannulas were secured with acrylic dental cement and a single anchor screw threaded into the cranium. Carprofen (5 mg/kg, subcutaneously) was used for postoperative analgesia (once daily for 2 days). Animals were allowed 1 week for recovery (housed one per cage) before testing. Microdialysis was performed as previously described by Lupinsky.[18] Probes were calibrated in artificial cerebrospinal fluid (26 mmol/L $NaHCO_3$, 3 mmol/L $NaH_2PO_4$, 1.3 mmol/L $MgCl_2$, 2.3 mmol/L $CaCl_2$, 3.0 mmol/L KCl, 126 mmol/L NaCl, 0.2 mmol/L L-ascorbic acid) containing 100 ng/ml aspartate, GLU, and GABA. *In vitro* probe recovery ranged from 14% to 19% at a flow rate of 2 μL/min. Computer-controlled microinfusion pumps were used to deliver perfusate to the probes, and the dialysate was collected from the fused silica outlet line (dead volume: 0.79 μL).

Microdialysis was performed under isoflurane anesthesia (2% isoflurane at 0.5 L/min oxygen flow). Two microdialysis probes (see Figures 4A and 4B) were inserted into the animals' indwelling guide cannula and perfused with sterile artificial cerebrospinal fluid (flow rate set at 1 μL/min). Samples were then taken at 20-minute intervals for 1 hour (baseline), followed by CEF (200 mg/kg) injection in the tail vein, while still collecting samples for 4 hours (challenge, Figure 1C). Each 20-μL dialysate sample was collected in a fraction vial preloaded with 1 μL of 0.25 mol/L perchloric acid to prevent analyte degradation and immediately stored at 4°C for subsequent analysis. After microdialysis, animal brains were dissected and stored in 4% paraformaldehyde and subsequently cryoprotected in a 30% sucrose solution. Brains were sliced in 20-μm-thick samples (coronal) and stained with cresyl violet (Nissl staining) for confirmation of probes placement.

### Lysate High-Performance Liquid Chromatography Analysis

Glutamate levels were determined as previously described by Lupinsky.[18] A high-performance liquid chromatography precolumn derivatization with electrochemical detection was used to determine glutamate levels. The chromatographic system consisted of an ESA pump (model 582) and an ESA injector (model 542) coupled to a Waters Xterra MS C18 3.0 × 50 mm 5 μm analytical column. The mobile phase was prepared as needed and consisted of 3.5% acetonitrile, 20% methanol, and 100 mmol/L sodium

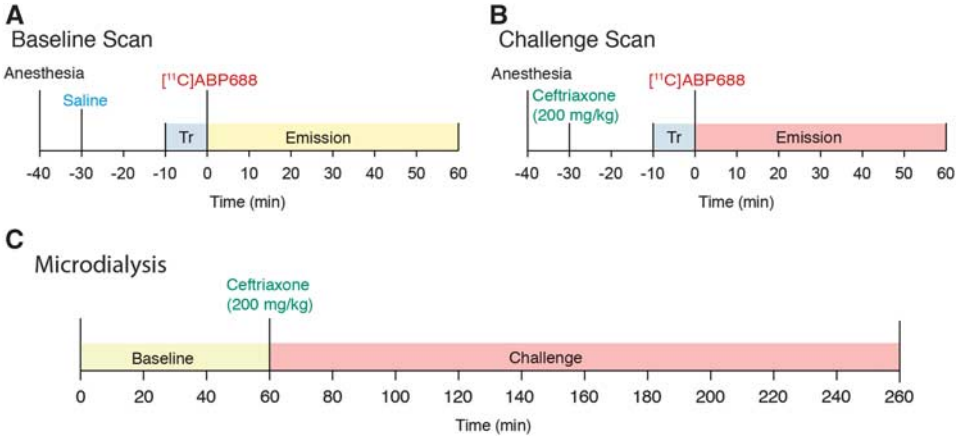


**Figure 1.** [$^{11}$C]ABP688 and ceftriaxone (CEF) challenge study design. (**A**) MicroPET baseline: rats received a saline tail vein injection 30 minutes before the scan, a 10-minute transmission (Tr) scan preceded the 60-minute emission scan; (**B**) MicroPET challenge: the same rats used for baseline, received a CEF tail vein injection (200 mg/kg) 30 minutes before the scan, a 10-minute Tr scan preceded the 60-minute emission scan; (**C**) Microdialysis: additional rats are used for microdialysis, a baseline microdialysis was performed during 60 minutes (three samples) followed by a CEF tail vein injection (200 mg/kg) and microdialysis challenge sampling during 200 minutes (10 samples). PET, positron emission tomography.

phosphate dibasic ($Na_2HPO_4$) adjusted to pH 6.7 with 85% phosphoric acid. The flow rate was set at 0.5 mL/min, and the electrochemical detector ESA Coularray 5600 A, Chelmsford, MA, USA) was set at potentials of +150 mV and +550 mV. Working standards (100 ng/mL) and derivatization reagents were prepared fresh daily from stock solutions and loaded with samples into a refrigerated (10°C) ESA autosampler (model 542, Chelmsford, MA, USA). Before injection onto the analytical column, each fraction was sequentially mixed with 20 $\mu$L of o-phthaldehyde (0.0143 mol/L) diluted with 0.1 mol/L sodium tetraborate and 20 $\mu$L of 3-mercaptopropionic acid (0.071 mol/L) diluted with $H_2O$ and allowed to react for 5 minutes. After each injection, the injection loop was flushed with 20% methanol to prevent contamination of subsequent samples. Under these conditions, the retention time for GLU was 2.4 minutes with a total run time of 30 minutes/sample. Chromatographic peak analysis was accomplished by

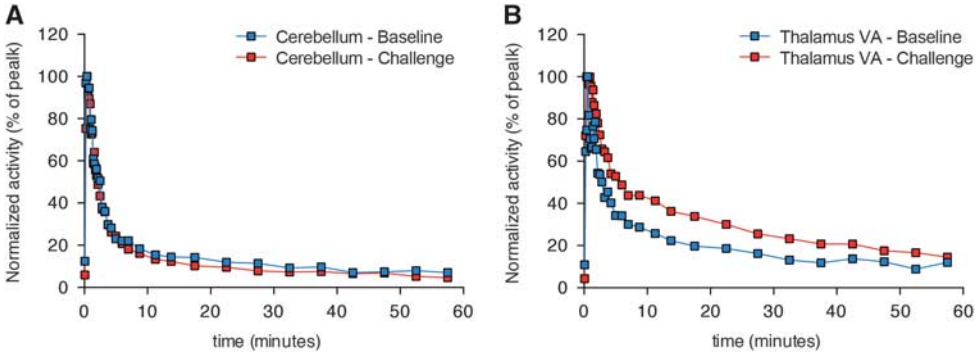


**Figure 2.** [11C]ABP688 time-activity curves (TACs) obtained from baseline and challenge conditions. (**A**) Baseline and post ceftriaxone TACs from the cerebellum (reference region) and (**B**) the thalamic VA nucleus (high-binding region) of a single rat. Blue squares represent baseline condition and red squares the challenge condition.

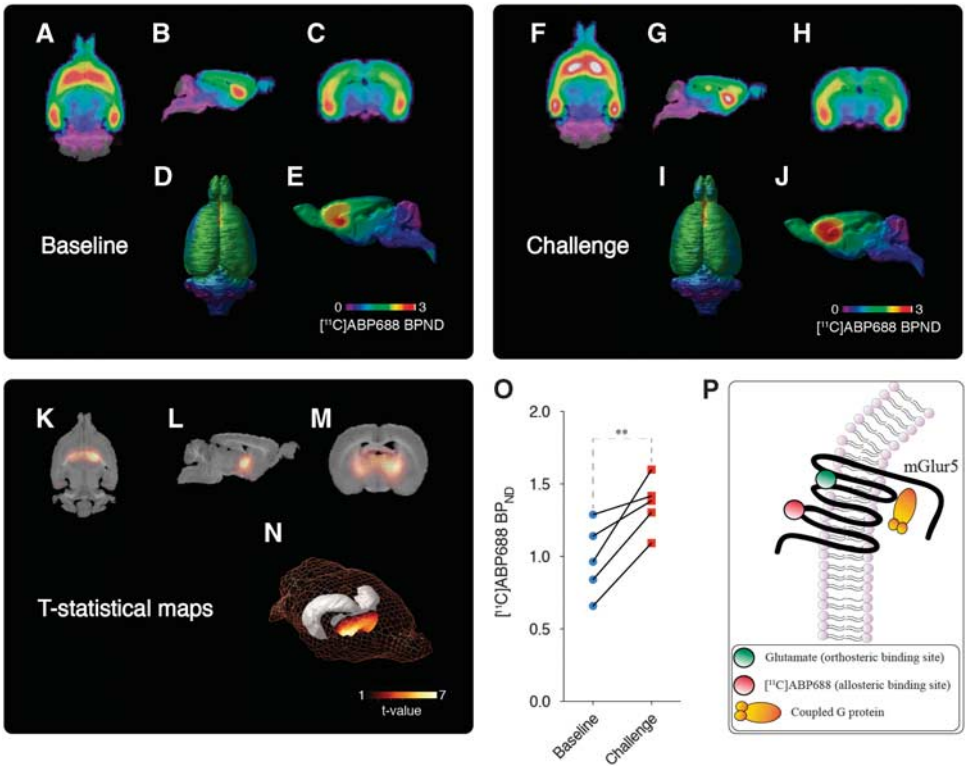


**Figure 3.** Baseline and ceftriaxone (CEF) challenge averaged [11C]ABP688 nondisplaceable binding potential ($BP_{ND}$). Averaged [11C]ABP688 $BP_{ND}$ images obtained during the baseline overlaid on a histologic template are shown in axial (**A**), sagittal (**B**), coronal (**C**), as well as dorsal (**D**) and mid-sagittal surface projections (**E**). Averaged [11C]ABP688 $BP_{ND}$ images obtained after CEF challenge overlaid on a histologic template are shown in axial (**F**), sagittal (**G**), coronal (**H**), as well as dorsal (**I**) and mid-sagittal surface projections (**J**). Statistical parametric images (t-stats contrast (CEF challenge > baseline)) overlaid on a histologic template are shown on axial view (**K**); sagittal view (**L**); coronal view (**M**); and rat brain 3D surface showing (**N**) peak t-stat region (the gray object represents hippocampal position in the 3D surface). Note group differences showing a symmetric cluster in the anterior thalamus, encompassing basal forebrain and posterior striatum with the local maxima at the thalamic VA. [11C]ABP688 $BP_{ND}$ in the local maxima, during baseline and challenge microPET scans (**O**). Schematic representation of [11C]ABP688 $BP_{ND}$ binding in the metabotropic glutamate receptor type 5 (mGlur5) allosteric site (**P**). Images represented as [11C]ABP688 $BP_{ND}$ and *t*-value. Graph represented as mean ± s.d., $n = 5$. $^{**}P < 0.01$. PET, positron emission tomography.

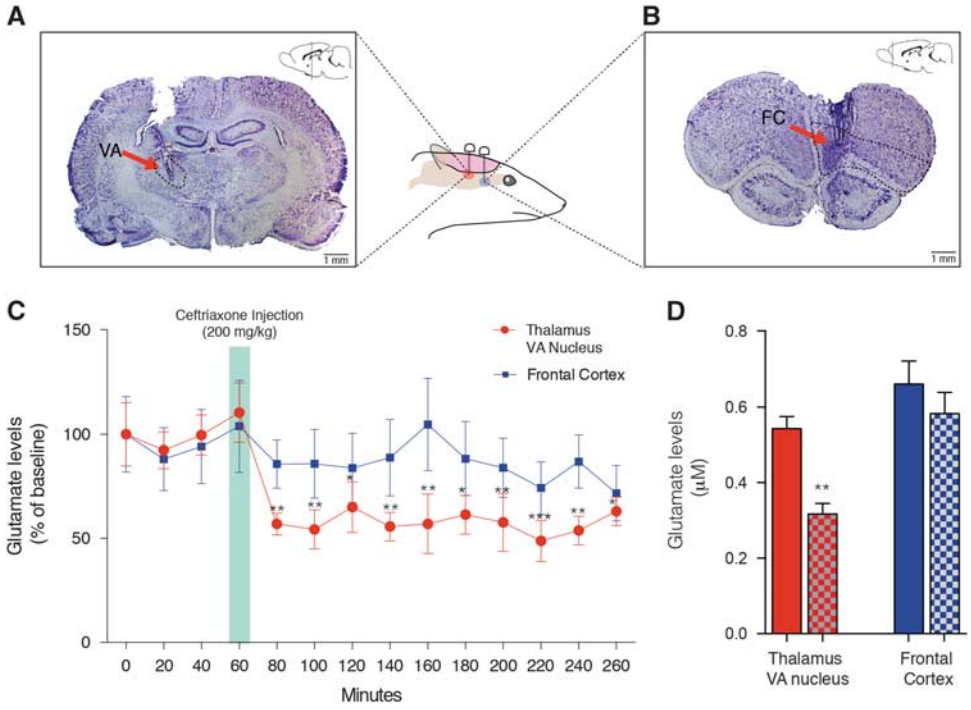


**Figure 4.** Ceftriaxone reduced levels of glutamate in the thalamic ventral nucleus but not in the frontal cortex (FC). (**A**) Histologic verification (cresyl violet) at VA (anteroposterior (AP): -1.88 mm, mediolateral (ML): 2.0 mm, dorsoventral (DV): 6.5 mm) microdialysis probes; (**B**) Histologic verification (cresyl violet) at FC (AP: 4.20 mm, ML: 1.0 mm, DV: 5.0 mm) microdialysis probes; (**C**) Levels of glutamate measured by microdialysis in the VA and in the FC during baseline (60 minutes) and challenge (200 minutes) conditions; (**D**) Comparison between levels of glutamate during baseline (solid bars) and challenge (checkered bars) at 60 minutes (the same duration as the PET scanning period). Data presented as mean ± s.e.m, $N = 6$. $^{*}P < 0.05$, $^{**}P < 0.01$, $^{***}P < 0.001$.

identification of unknown peaks in a sample matched according to retention times from known standards using ESA's CoulArray software.

### Statistical Analysis

A paired Student's *t*-test was used to calculate differences in the [11C]ABP688 $BP_{ND}$ between challenge and baseline. Comparisons between baseline and challenge were conducted at the voxel level using t-statistic analyses (RMINC, https://launchpad.net/rminc). Regions showing high specific binding were adjusted for a statistical cluster-wise threshold of $P < 0.05$, and corrected for multiple comparisons using random field theory.[19] For microdialysis, two-way ANOVA with repeated measures followed by Bonferroni correction was used. Differences were considered statistically significant at $P < 0.05$.

## RESULTS

### Ceftriaxone Challenge Increased [11C]ABP688 $BP_{ND}$ with Peak Effect in the Thalamic Ventral Anterior Nucleus

Figure 2 shows the representative time-activity curves of reference region (cerebellum, Figure 2A) and of a high-binding region (thalamic VA nucleus, Figure 2B). Averaged $BP_{ND}$ images showed consistent brain uptake of [11C]ABP688, and no global differences between baseline and challenge (baseline: 1.06 ± 0.24; challenge: 1.14 ± 0.26; $t_{(4)} = 0.5135$, $P = 0.6347$; Figures 3A and 3J). Voxel-based analysis showed a large bilateral symmetric cluster with increased [11C]ABP688 $BP_{ND}$ in the thalamus, with peak effect in the thalamic ventral nucleus (VA) (peak $t_{(4)} = 6.78$, $P = 0.0025$, Figures 3K–3N) after the challenge with CEF. Paired *t*-test showed a significant increase in the [11C]ABP688 $BP_{ND}$ in the VA (local maxima) after challenge with CEF ($t_{(4)} = 5.295$, $P = 0.0061$, baseline: 0.9781 ± 0.24; challenge: 1.379 ± 0.08 Figure 3O).

### Ceftriaxone Evoked Glutamate Reductions in the Thalamic Ventral Nucleus

Repeated measures two-way ANOVA revealed an effect of drug ($F_{(13,130)} = 5.379$, $P = 0.0001$) but not of region ($F_{(1,10)} = 1.373$, $P = 0.2685$). A significant interaction between drug and region ($F_{(13,130)} = 2.109$, $P = 0.0175$) was observed. Bonferroni *post hoc* analysis revealed decreased glutamate concentrations after challenge in the VA ($P_{(range)} = 0.0004$ to 0.0314) but not in the FC ($P_{(range)} = 0.2526$ to 0.999; Figure 4C). Comparison between averages of baseline and CEF challenge during the scan period also showed decreased extracellular levels of glutamate in the VA ($t_{(5)} = 4.183$, $P = 0.0086$), but not in the FC ($t_{(5)} = 1.482$, $P = 0.20$; Figure 4D).

## DISCUSSION

The present study showed for the first time the effect of the reduction of extracellular glutamate levels, using a GLT-1 pharmacological challenge with CEF, on PET [11C]ABP688 binding.

In a previous study, we validated the cerebellum as a suitable reference region for the quantification of mGluR5 availability using [11C]ABP688 in rats, via *in vivo* (microPET) and *in vitro* (autoradiography) techniques. Additionally, we performed a blood-based pharmacokinetics analysis and a blocking study with 1,2-methyl-6-(phenylethynyl)-pyridine, an antagonist of mGluR5 allosteric binding site and a competitor of [11C]ABP688.[13] Furthermore, we evaluated the reproducibility of [11C]ABP688 binding in a test-retest study and examined several pharmacokinetic models for determination of binding potential ($BP_{ND}$), showing that the simplified reference tissue model is the pharmacokinetic model that presents lowest variability.[20]

These validation studies allowed us to proceed with a pharmacological challenge aiming to identify the impact of reduced

glutamate concentrations on [11C]ABP688 binding in rats. Here, we show that the acute CEF challenge increased [11C]ABP688 binding in the thalamic VA. Beyond the considerable expression levels of GLT-1,[21] the thalamic VA receives massive glutamatergic afferents from the cerebellum and basal ganglia[22] and drives several connections with prefrontal, premotor, and motor cortices, a piece of the so-called thalamocortical network.[23,24]

Interestingly, [11C]ABP688 binding to the transmembrane allosteric site instead of orthosteric binding site of glutamate (Figure 3P) is highly dependent on the tertiary and quaternary receptor conformations.[25] Additionally, mGluR5 can assume oligomeric or heteromeric forms,[26–28] which may have an impact on the availability of the allosteric site. One could also argue that glutamate levels alter mGluR5 conformational states. In fact, affinity shift in the receptor–radioligand interactions is a phenomenon already described in the case of dopamine D2 receptors, where an amphetamine challenge altered the affinity of a D2 PET radiopharmaceutical.[29–31]

Guided by [11C]ABP688 microPET data, a microdialysis study was performed to confirm the reduction of glutamate levels in the VA. As expected, since [11C]ABP668 binding was not altered in the cerebral cortex, levels of glutamate in the FC (used as a control region) remained stable after CEF injection. In contrast, 20 minutes after CEF injection glutamate levels were reduced in the VA. However, the reason why this thalamic region is the first to be affected by CEF since GLT-1 and mGluR5 are expressed in almost all brain regions remains unknown and requires further investigation. One could argue that the differential expression and splice variants of GLT-1 in diverse brain regions may yield distinct activation by CEF.[32,33] Further studies are necessary to validate this observation; however, it seems unlikely that the changes in [11C]ABP688 binding are the result of a direct displacement by CEF, since CEF does not bind to the mGluR5 allosteric site. In fact, further methodological developments are necessary to better understand noncompetitive interactions using PET. Altogether, our results support a theoretical framework in which synaptic glutamate concentrations anticorrelate with [11C]ABP688 binding (i.e., low levels of glutamate will produce increased [11C]ABP688 binding and high levels of glutamate decreased [11C]ABP688 binding). Interestingly, two recent studies showed that [11C]ABP688 PET was capable of identifying reductions in mGluR5 availability in patients with major depressive disorder,[34] and in an epilepsy rat model.[35] On the basis of our assumptions, reduced [11C]ABP688 PET binding in this study may indicate increased glutamate levels, a possible sign of early excitotoxicity. This seems reasonable since excitotoxicity is an important pathological entity in both major depression[36] and epilepsy.[37]

In summary, molecular imaging using [11C]ABP688 seems to constitute a valuable tool for noninvasive and *in vivo* assessment of glutamatergic neurotransmission. Studies encompassing a wide range of clinical populations displaying glutamate-related neurologic and neuropsychiatric conditions are necessary to fully evaluate the feasibility and potential of [11C]ABP688 for measuring clinically-relevant glutamatergic fluctuations. If these clinical studies succeed, then [11C]ABP688 PET imaging will offer the opportunity of identifying glutamate abnormalities (e.g., brain excitotoxicity), which may allow for the development of glutamate-based disease signatures and for the evaluation of glutamate focused therapies.

## AUTHOR CONTRIBUTIONS

ERZ and PRN were responsible for the design, drafting and revising the manuscript. ERZ and MJP were responsible for imaging processing and analysis. AL was responsible for drafting and revising the manuscript. ERZ, Arturo A and AA were responsible for microPET procedures and histology. ERZ, Arturo A and LM were responsible for microdialysis procedures. ESS and JPS were responsible for the radiochemistry. AG, SG and PRN critically revised the final version of the manuscript. PRN and AG were responsible for overseeing the entire PET and microdialysis procedures, respectively.

## DISCLOSURE/CONFLICT OF INTEREST

The authors declare no conflict of interest.

## REFERENCES

1 Schaeffer E, Duplantier A. Glutamate and neurodegenerative fisease. In: Dominguez C (ed.) *Neurodegenerative diseases* vol. 6. Springer: Berlin, Heidelberg, 2010 pp 91–147.
2 Danbolt NC. Glutamate uptake. *Prog Neurobiol* 2001; **65**: 1–105.
3 Mark LP, Prost RW, Ulmer JL, Smith MM, Daniels DL, Strottmann JM *et al.* Pictorial review of glutamate excitotoxicity: fundamental concepts for neuroimaging. *AJNR Am J Neuroradiol* 2001; **22**: 1813–1824.
4 Mehta A, Prabhakar M, Kumar P, Deshmukh R, Sharma PL. Excitotoxicity: bridge to various triggers in neurodegenerative disorders. *Eur J Pharmacol* 2013; **698**: 6–18.
5 Jacobs AH, Li H, Winkeler A, Hilker R, Knoess C, Ruger A *et al.* PET-based molecular imaging in neuroscience. *Eur J Nucl Med Mol Imaging* 2003; **30**: 1051–1065.
6 Ametamey SM, Kessler LJ, Honer M, Wyss MT, Buck A, Hintermann S *et al.* Radiosynthesis and preclinical evaluation of 11C-ABP688 as a probe for imaging the metabotropic glutamate receptor subtype 5. *J Nucl Med* 2006; **47**: 698–705.
7 Miyake N, Skinbjerg M, Easwaramoorthy B, Kumar D, Girgis RR, Xu X *et al.* Imaging changes in glutamate transmission in vivo with the metabotropic glutamate receptor 5 tracer [11C] ABP688 and N-acetylcysteine challenge. *Biol Psychiatry* 2011; **69**: 822–824.
8 Sandiego CM, Nabulsi N, Lin SF, Labaree D, Najafzadeh S, Huang Y *et al.* Studies of the metabotropic glutamate receptor 5 radioligand [(1)(1)C]ABP688 with N-acetylcysteine challenge in rhesus monkeys. *Synapse* 2013; **67**: 489–501.
9 Wyckhuys T, Verhaeghe J, Wyffels L, Langlois X, Schmidt M, Stroobants S *et al.* N-acetylcysteine- and MK-801-induced changes in glutamate levels do not affect in vivo binding of metabotropic glutamate 5 receptor radioligand 11C-ABP688 in rat brain. *J Nucl Med* 2013; **54**: 1954–1961.
10 Rothstein JD, Patel S, Regan MR, Haenggeli C, Huang YH, Bergles DE *et al.* Beta-lactam antibiotics offer neuroprotection by increasing glutamate transporter expression. *Nature* 2005; **433**: 73–77.
11 Rasmussen BA, Baron DA, Kim JK, Unterwald EM, Rawls SM. beta-Lactam antibiotic produces a sustained reduction in extracellular glutamate in the nucleus accumbens of rats. *Amino Acids* 2011; **40**: 761–764.
12 Thone-Reineke C, Neumann C, Namsolleck P, Schmerbach K, Krikov M, Schefe JH *et al.* The beta-lactam antibiotic, ceftriaxone, dramatically improves survival, increases glutamate uptake and induces neurotrophins in stroke. *J Hypertens* 2008; **26**: 2426–2435.
13 Elmenhorst D, Minuzzi L, Aliaga A, Rowley J, Massarweh G, Diksic M *et al.* In vivo and in vitro validation of reference tissue models for the mGluR(5) ligand [(11)C] ABP688. *J Cereb Blood Flow Metab* 2010; **30**: 1538–1549.
14 Rubins DJ, Melega WP, Lacan G, Way B, Plenevaux A, Luxen A *et al.* Development and evaluation of an automated atlas-based image analysis method for microPET studies of the rat brain. *Neuroimage* 2003; **20**: 2100–2118.
15 Lammertsma AA, Hume SP. Simplified reference tissue model for PET receptor studies. *Neuroimage* 1996; **4**(3 Pt 1): 153–158.
16 Gunn RN, Lammertsma AA, Hume SP, Cunningham VJ. Parametric imaging of ligand-receptor binding in PET using a simplified reference region model. *NeuroImage* 1997; **6**: 279–287.
17 Paxinos G, Watson C. *The rat brain in stereotaxic coordinates*, 4th ed. Academic Press: San Diego, 1998.
18 Lupinsky D, Moquin L, Gratton A. Interhemispheric regulation of the medial prefrontal cortical glutamate stress response in rats. *J Neurosci* 2010; **30**: 7624–7633.
19 Worsley KJ, Marrett S, Neelin P, Vandal AC, Friston KJ, Evans AC. A unified statistical approach for determining significant signals in images of cerebral activation. *Hum Brain Mapp* 1996; **4**: 58–73.
20 Elmenhorst D, Aliaga A, Bauer A, Rosa-Neto P. Test-retest stability of cerebral mGluR(5) quantification using [(1)(1)C]ABP688 and positron emission tomography in rats. *Synapse* 2012; **66**: 552–560.
21 Ozawa T, Nakagawa T, Shige K, Minami M, Satoh M. Changes in the expression of glial glutamate transporters in the rat brain accompanied with morphine dependence and naloxone-precipitated withdrawal. *Brain research* 2001; **905**: 254–258.
22 Kuramoto E, Fujiyama F, Nakamura KC, Tanaka Y, Hioki H, Kaneko T. Complementary distribution of glutamatergic cerebellar and GABAergic basal ganglia afferents to the rat motor thalamic nuclei. *Eur J Neurosci* 2011; **33**: 95–109.

23 Zikopoulos B, Barbas H. Parallel driving and modulatory pathways link the prefrontal cortex and thalamus. *PLoS One* 2007; **2**: e848.
24 Ngomba RT, Santolini I, Salt TE, Ferraguti F, Battaglia G, Nicoletti F *et al.* Metabotropic glutamate receptors in the thalamocortical network: strategic targets for the treatment of absence epilepsy. *Epilepsia* 2011; **52**: 1211–1222.
25 Changeux J-P, Edelstein SJ. Allosteric mechanisms of signal transduction. *Science* 2005; **308**: 1424–1428.
26 Canela L, Fernandez-Duenas V, Albergaria C, Watanabe M, Lluis C, Mallol J *et al.* The association of metabotropic glutamate receptor type 5 with the neuronal Ca2+-binding protein 2 modulates receptor function. *Journal of neurochemistry* 2009; **111**: 555–567.
27 Cabello N, Gandia J, Bertarelli DC, Watanabe M, Lluis C, Franco R *et al.* Metabotropic glutamate type 5, dopamine D2 and adenosine A2a receptors form higher-order oligomers in living cells. *Journal of neurochemistry* 2009; **109**: 1497–1507.
28 Romano C, Yang WL, O'Malley KL. Metabotropic glutamate receptor 5 is a disulfide-linked dimer. *J Biol Chem* 1996; **271**: 28612–28616.
29 Narendran R, Hwang DR, Slifstein M, Talbot PS, Erritzoe D, Huang Y *et al.* In vivo vulnerability to competition by endogenous dopamine: comparison of the D2 receptor agonist radiotracer (-)-N-[11C]propyl-norapomorphine ([11C]NPA) with the D2 receptor antagonist radiotracer [11C]-raclopride. *Synapse* 2004; **52**: 188–208.
30 Seneca N, Finnema SJ, Farde L, Gulyas B, Wikstrom HV, Halldin C *et al.* Effect of amphetamine on dopamine D2 receptor binding in nonhuman primate brain: a comparison of the agonist radioligand [11C]MNPA and antagonist [11C]raclopride. *Synapse* 2006; **59**: 260–269.
31 Wilson AA, McCormick P, Kapur S, Willeit M, Garcia A, Hussey D *et al.* Radiosynthesis and evaluation of [11C]-(+)-4-propyl-3,4,4a,5,6,10b-hexahydro-2H-naphtho[1,2-b][1,4]oxazin-9-ol as a potential radiotracer for in vivo imaging of the dopamine D2 high-affinity state with positron emission tomography. *Journal of medicinal chemistry* 2005; **48**: 4153–4160.
32 Reye P, Sullivan R, Scott H, Pow DV. Distribution of two splice variants of the glutamate transporter GLT-1 in rat brain and pituitary. *Glia* 2002; **38**: 246–255.
33 Torp R, Hoover F, Danbolt NC, Storm-Mathisen J, Ottersen OP. Differential distribution of the glutamate transporters GLT1 and rEAAC1 in rat cerebral cortex and thalamus: an in situ hybridization analysis. *Anat Embryol (Berl)* 1997; **195**: 317–326.
34 Deschwanden A, Karolewicz B, Feyissa AM, Treyer V, Ametamey SM, Johayem A *et al.* Reduced metabotropic glutamate receptor 5 density in major depression determined by [(11)C]ABP688 PET and postmortem study. *Am J Psychiatry* 2011; **168**: 727–734.
35 Choi H, Kim YK, Oh SW, Im HJ, Hwang do W, Kang H *et al.* In Vivo Imaging of mGluR5 Changes during Epileptogenesis Using [11C]ABP688 PET in Pilocarpine-Induced Epilepsy Rat Model. *PLoS One* 2014; **9**: e92765.
36 Hashimoto K. Emerging role of glutamate in the pathophysiology of major depressive disorder. *Brain Res Rev* 2009; **61**: 105–123.
37 Meldrum BS. The role of glutamate in epilepsy and other CNS disorders. *Neurology* 1994; **44**(11 Suppl 8): S14–S23.